Carbohydrate-Based Micelle Clusters Which Enhance Hydrophobic Drug Bioavailability by Up to 1 Order of Magnitude

Xioazhong Qu,[†] Vitaliy V. Khutoryanskiy,[†] Ailsa Stewart,[†] Samina Rahman,[†] Brigitte Papahadjopoulos-Sternberg,[‡] Christine Dufes,[§] Dave McCarthy,[∥] Clive G. Wilson,[†] Robert Lyons,[⊥] Katharine C. Carter,[#] Andreas Schätzlein,[§] and Ijeoma F. Uchegbu*[,†]

Department of Pharmaceutical Sciences, University of Strathclyde, 27 Taylor Street, Glasgow G4 0NR, U.K., NanoAnalytical Laboratory, 3951 Sacramento Street, San Francisco, California 94118, Cancer Research UK Centre for Medical Oncology and Applied Pharmacology, University of Glasgow, Garscube Estate, Switchback Road, U.K., Electron Microscopy Unit, School of Pharmacy, University of London, 29-39 Brunswick Square, London WC1N 1AX, U.K., Allergan, Inc., 2525 Dupont Drive, Irvine, California 92623, and Department of Immunology, University of Strathclyde, 27 Taylor Street, Glasgow G4 0NR, U.K.

Received April 25, 2006; Revised Manuscript Received August 24, 2006

Amphiphilic chitosan-based polymers (M_w < 20 kDa) self-assemble in aqueous media at low micromolar concentrations to give previously unknown micellar clusters of 100−300 nm in size. Micellar clusters comprise smaller 10−30 nm aggregates, and the nanopolarity/drug incorporation efficiency of their hydrophobic domains can be tailored by varying the degree of lipidic derivatization and molecular weight of the carbohydrate. The extent of drug incorporation by these novel micellar clusters is 1 order of magnitude higher than is seen with triblock copolymers, with molar polymer/drug ratios of 1:48 to 1:67. On intravenous injection, the pharmacodynamic activity of a carbohydrate propofol formulation is increased by 1 order of magnitude when compared to a commercial emulsion formulation, and on topical ocular application of a carbohydrate prednisolone formulation, initial drug aqueous humor levels are similar to those found with a 10-fold dose of prednisolone suspension.

Introduction

The presence of both polar and apolar segments in a molecule allows the manipulation of immiscible liquids in a manner that is applicable to a wide variety of processes: ranging from the use of detergents for environmental clean up activities to the processing of foods. In the pharmaceutical industry, the formulation of drugs that are immiscible with water is often fraught with failure[1,2] despite the availability of amphiphilic compounds with approved excipient status.[3] Micellar phases are often used to solubilize drugs in aqueous media, and the stability of the drug-solubilizing micellar core is a function of its critical micellar concentration (cmc, eq 1)—the concentration at which micellar aggregates begin to form:

$$\Delta G^0_{\text{micellization}} = RT \ln X_{\text{cmc}} \tag{1}$$

Here $\Delta G^0_{micellization}$ = the standard free energy of micellization, R = the gas constant, T = temperature, and X_{cmc} = the critical micelle concentration in mole fraction units. A lower cmc leads to a more negative $\Delta G^0_{\text{micellization}}$ and thus favors micellization. Pharmaceutically approved low molecular weight surfactants[4] and block copolymers[5−7] typically possess cmc values in the mM concentration range and are inefficient in carrying hydrophobic drugs as molar amphiphile/drug ratios are typically in excess of 10:1 and frequently extend to 1000:1.[4,8−10] The solubilization of drugs within micellar cores for a fixed mole of solubilizing micelle is dependent on factors such as the log P of the solubilizate,[11] molecular volume of the solubilizate,[11] and relative size of the hydrophobic nanodomain formed by the association colloid:[12,13]

$$\text{P} = \frac{C_o}{C_w} \tag{2}$$

Here C_o and C_w are the drug concentrations in the organic and aqueous phases, respectively, after drug partitioning between organic and aqueous phases. log P is a measure of the hydrophobicity of a drug. A high log P/molar volume ratio favors partitioning into micelles, and a large hydrophobic volume within the micelle favors the encapsulation of drugs within the micelle. Increasing the hydrophobic volume of a particle may be achieved by increasing the aggregation number of the individual monomers to yield larger particles, and this is thus a possible means of increasing the level of drug that may be solubilized within colloidal aggregates. However care must be taken to avoid excessive aggregation which would present as precipitation of the colloid-forming molecules and the drug. The use of larger aggregates (>100 nm), as opposed to the smaller conventional low molecular weight amphiphile micelles (12−36 nm[14-16]), is the approach that has been taken here. This has led to three surprising findings: (a) Carbohydrate amphiphiles aggregate into a hierarchically organized cluster

* To whom correspondence should be addressed. E-mail: i.f.uchegbu@strath.ac.uk.
[†] Department of Pharmaceutical Sciences, University of Strathclyde.
[‡] NanoAnalytical Laboratory.
[§] Cancer Research UK Centre for Medical Oncology and Applied Pharmacology, University of Glasgow.
[∥] School of Pharmacy, University of London.
[⊥] Allergan, Inc.
[#] Department of Immunology, University of Strathclyde.

10.1021/bm0604000 CCC: $33.50
Published on Web 11/07/2006

of individual aggregates. (b) These micellar clusters transform to stable nanoparticles with molar polymer/hydrophobic drug ratios as high as 1:67 (polymer, drug weight ratios as low as 0.8:1), $20^{17}-200$ times the level seen with the Pluronic block copolymers. (c) These micellar clusters improve the transfer of drugs across biological barriers by 1 order of magnitude. Two drugs with very different log P values were chosen to illustrate the capability of this new system: propofol (log P = 4.1) and prednisolone (log P = 1.4).

Although work on the self-assembly and pharmaceutical application of block copolymers has been reported,[18−22] no bioavailability gains have been reported with the current class of polymers: amphiphilic polymers bearing hydrophobic grafts.[23−25] While both block copolymer and grafted polymer amphiphiles self-assemble into polymeric micelles,[5,26] vesicles,[27,28] and dense amorphous nanoparticles,[26,29,30] there are profound differences in the self-assembly of these two types of polymers into soluble micellar aggregates, with the grafted polymers able to produce important bioavailability gains as described below.

Methods

Synthesis of Quaternary Ammonium Palmitoyl Glycol Chitosan. Quaternary ammonium palmitoyl glycol chitosan (GCPQ) samples were synthesized using a modification of the method previously reported,[24] as described below. All reagents were used as received and supplied by Sigma Aldrich Co., U.K., unless otherwise stated. Organic solvents were supplied by the Department of Pure and Applied Chemistry, University of Strathclyde. Glycol chitosan (GC, $M_w \sim 250$ kDa) with a degree of acetylation below the level of detection using ^{1}H NMR (signal at 2 ppm) was degraded for 48 h by heating at 50 °C in a solution of hydrochloric acid (4 M)[27] to give 10−15 kDa GC samples. Alternatively 4 kDa GC samples were prepared by adapting a previously published method of GC degradation.[31] GC ($M_w \sim 250$ kDa, 1 g) was dissolved in acetic acid (2.5% v/v, 50 mL). Dissolved oxygen was removed by bubbling N_2 gas through the solution for 5 min. After cooling of the sample to 0−4 °C, a freshly prepared solution of $NaNO_2$ (9.5 mg mL^{-1}, 2 mL) was added, and the reaction was allowed to proceed for 15 h at 4 °C in the dark and without stirring. The product was neutralized with concentrated aqueous ammonia. To the resulting mixture was added $NaBH_4$ (20 mg) in divided portions, and the reaction mixture was once again left stirring overnight at room temperature. At the end of this period the product was carefully precipitated by adding acetone (150 mL) at room temperature. The resulting precipitate was separated by centrifugation (9000g × 10 min), washed three times with methanol (50 mL), redissolved in water, and dialyzed exhaustively as described below, with the dialyzate freeze-dried. The yield of degraded GC was 400 mg.

Degraded GC (300 mg) was dissolved in an aqueous sodium bicarbonate solution (0.057 M), a solution of palmitic acid *N*-hydroxysuccinimide (120 mL) added at the level given in Table 1, and the mixture stirred for 72 h. Ethanol was removed by evaporation under reduced pressure and the reaction mixture extracted with diethyl ether (3 × 100 mL). The crude palmitoyl glycol chitosan (PGC) was dissolved in an *N*-methyl pyrrolidone solution of sodium iodide (0.011 M, 90 mL) by stirring overnight. To this solution was added an ethanolic solution of sodium hydroxide (0.25 M, 18 mL) and methyl iodide at the level indicated in Table 1. The mixture was stirred under nitrogen gas at 36 °C for 4 h and the product precipitated in diethyl ether (400 mL) and washed twice with diethyl ether (2 × 300 mL). Finally the quaternized product was dissolved in water (100 mL) and dialyzed exhaustively against an aqueous sodium chloride solution (0.1 M, 5 L) to give a protonated polymer (chitosan, p$K_a \sim 7$) or an aqueous solution (5 L) containing sodium bicarbonate (0.01 M) and sodium chloride (0.1 M), the latter giving a deprotonated polymer. Both dialysis media described above were changed 3 times (over 4.5 h) and followed by

Table 1. Polymer Samples

sample[a]	M_w of glycol chitosan starting material (kDa)	Initial gravimetric feed ratio of PNS:GC	molar proportn of palmitoyl groups/ monomer (L)	init gravimetric feed ratio of methyl iodide:GC	molar proportn of quaternary ammonium groups/ monomer (Q)	HI (Q/L)	HLB	cmc (g L^{-1}/ μM)	carbohydrate aggregate mean particle size/ polydispersity	mean particle size after filtratn/ polydispersity	mean particle size/polydispersity after drug loading and filtratn	final methyl orange $\lambda_{max.}$ (nm)
A1	15	0.26	0.0215	5.02	0.1074	5.00	19.7	1.76/106	259/0.16	184/0.09	163/0.07	442
A2	15	2.11	0.1508	5.02	0.1649	1.09	17.9	0.17/8.93	241/0.14	201/0.12	nd	426
A3	15	1.06	0.1028	9.58	0.2015	2.22	18.5	0.09/4.9	200/0.27	178/0.22	nd	428
A4	15	0.26	0.0196	14.14	0.1189	5.69	19.7	0.80/47.9	303/0.37	172/0.06	170/0.13	438
A5	15	2.11	0.117	14.14	0.1300	1.11	18.3	0.11/5.9	230/0.39	163/0.33	209/0.10	426
B1	19	2.11	0.123	9.58	0.221	1.80						
A7	15	0.79	0.168	18.24	0.743	4.4	17.8	0.08/4.0	348	147	154	432
A6	15	1.58	0.134	9.13	0.337	2.3	18.0	0.11/6.1	315	152		429
C1	10	2.11	0.134	14.14	0.134	1.00	18.0					
C2	10	2.11	0.160	14.14	0.137	1.17	17.6					
C3	10	2.11	0.185	14.14								
C4	10	0.26	0.020	14.14	0.119	5.95	19.7					
D1	4	2.11	0.1510	14.14	0.1263	0.84	17.7	0.363/76.8		132/0.63		432

[a] A series of polymers, M_w of GC starting material ~ 15kDa; B series of polymers, M_w of GC starting material ~ 19 kDa; C series of polymers, M_w of GC starting material ~ 10 kDa; D series of polymers, M_w of GC starting material ~ 4 kDa.

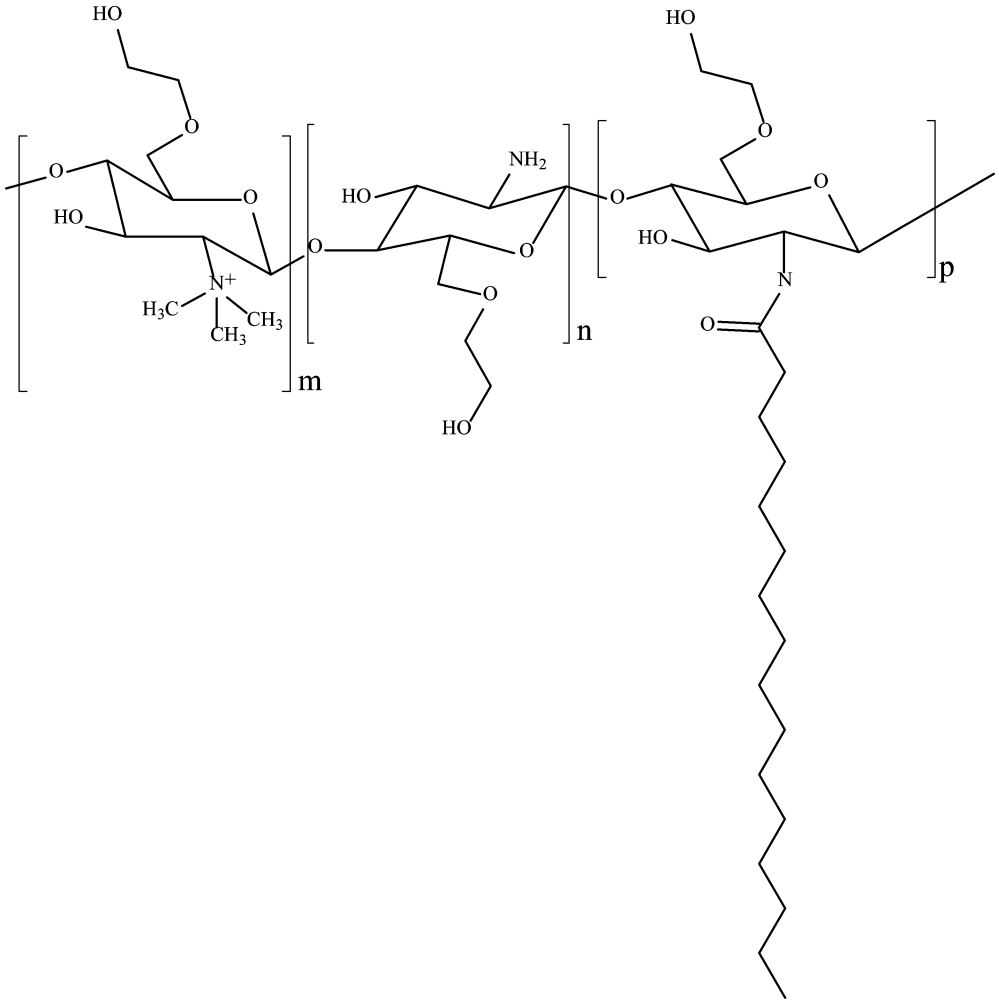

Figure 1. Quaternary ammonium palmitoyl glycol chitosan.

dialysis against water (5 L) with 6 changes (over 24 h). The synthetic yield for all polymers was ~120 mg. Synthesized polymers are shown in Table 1. Protonated and deprotonated versions of C1 (Table 1) were prepared. All other polymers were dialyzed against water (5 L with 6 changes over 24 h) and passed through an ion exchange column equilibrated with chloride ions (IRA 93 Cl-1)[24] prior to freeze drying.

The molecular weight of degraded GC was determined by gel permeation chromatography−multiangle laser light scattering[27] and the level of both palmitoylation and methylation determined by ^{1}H NMR by comparing the palmitoyl methyl protons (0.8 ppm, palmitoyl) and the quaternary ammonium methyl protons (3.35 ppm, quaternary ammonium glycol chitosan) respectively with the sugar methine protons (3.1 and 3.5−5.5 ppm).[24] The hydrophobicity index (HI) was calculated using

$$\mathrm{HI} = \frac{Q}{L} \tag{3}$$

where Q = molar fraction of quaternary ammonium groups/monomer and L = molar fraction of palmitoyl groups/monomer. This index was used as it best refers adequately to the synthetic controls achievable with these carbohydrate amphiphiles. Also an approximation of the hydrophilic lipophilic balance (HLB)[4,32] was made using

$$\mathrm{HLB} = \frac{M_1Q + \{M_2[1-(Q+L)]\} + M_3L}{M_4L + M_1Q + \{M_2[1-(Q+L)]\} + M_3L}\left(\frac{100}{5}\right) \tag{4}$$

where M_1 = molecular weight of quaternary ammonium sugar monomer, M_2 = molecular weight of amino sugar monomer, M_3 = molecular weight of CH_2CO- amino sugar monomer, and M_4 = molecular weight of tetradecyl moiety.

Polymer Aggregation and Drug Encapsulation. Methyl orange serves as a solvatochromic probe by undergoing a hypsochromic shift of its long-wavelength band on movement from a polar to a nonpolar domain,[26,33] such as that resulting from polymer aggregation.[26] Alkaline solutions of methyl orange were used to probe for polymer aggregation, by measuring the degree of the hypsochromic shift with increase in polymer aqueous concentration.[26] The cmc was taken as the first inflection point in the methyl orange wavelength of maximum absorbance−concentration curve. GCPQ NMR and GC GPC-MALLS data were used to calculate the molecular weight of the polymers to obtain molar cmc data. Photon correlation spectroscopy was used to record aggregate size before and after filtration (0.45 μm),[29] and both freeze fracture electron microscopy[34] and negative stained transmission electron microscopy[27] were used to record images of the aggregates.

Drug loading on the aggregates was achieved by probe sonicating[29] a mixture of the drug (prednisolone or propofol) and the polymer (GCPQ or F127) in aqueous media. Drug levels contained in the aggregates were measured after filtration of the aggregates (0.45 μm) and analysis by high-performance liquid chromatography (HPLC). Polymer/prednisolone samples were filtered, diluted with the mobile phase (water/acetonitrile 640 mL:360 mL), and chromatographed (20 μL) over a reverse phase 3.5 μm C18 column symmetry (4.6 × 75 mm, Waters Instruments, U.K.) at a mobile phase flow rate of 1 mL min^{-1}. Chromatography was achieved using a Waters 515 isocratic pump and a Waters 717 autosampler, and sample detection was achieved using a Waters 486 variable wavelength ultraviolet wavelength detector (λ = 243 nm). The internal standard was 6α-methyl prednisolone (50

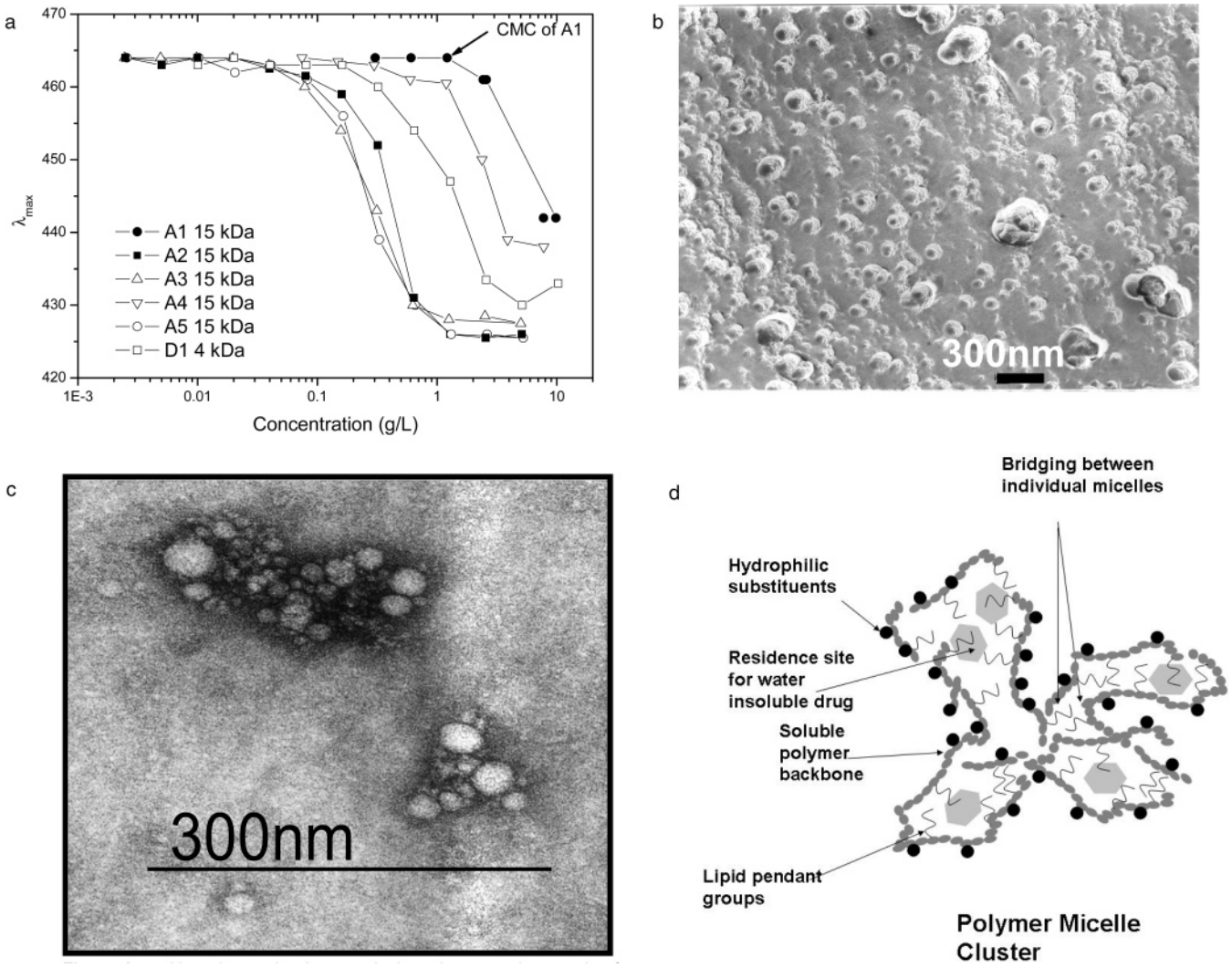

Figure 2. (a) Effect of polymer hydrophobicity and molecular weight on polymer aggregation as probed by measuring the hypsochromic shift in methyl orange solutions. On location within an apolar environment methyl orange undergoes a hypsochromic shift. Polymer cmc is determined as the first inflection point (arrowed for A1). For polymer details, hydrophobicity index (HI), approximated hydrophobic lipophilic balance (HLB), and cmc values, see Table 1. Molecular weight values refer to the molecular weight of the glycol chitosan starting material. (b) Freeze fracture electron micrograph of E5 (5.0 mg mL^{-1}) in water. (c) Negative stained transmission electron micrograph of C5 (5 mg mL^{-1}) in water. (d) Schematic representation of the self-assembled polymer micelle cluster.

Table 2. Drug Loading

drug	log *P*	amphiphile	M_w (kDa)	HLB	cmc (μM)	mol drug encapsulated/ mol of polymer	drug concn (g L^{-1})
propofol	4.1	C1	11.7	18.0		48	3.6
		D1	4.7	17.7	76.8	3.2	0.61
		F127	12.6	14	550[6]	3[17]	1.78
		2-hydroxypropyl-β-cyclodextrin	1.3			0.75[10]	38.7
prednisolone	1.4	A7	19.9	17.8	4.0	67	1.2
		F127	12.6	14	550	0.21	0.5

ng mL^{-1}), the limit of detection was 5 ng mL^{-1}, and the linear peak area ratio−concentration curve over the range 10−250 ng mL^{-1} had a correlation coefficient of 0.9991. Polymer/propofol samples were filtered (0.45 μm), diluted with the mobile phase (water/methanol 200 mL:800 mL), and chromatographed (20 μL) over an ODS2 5 μm column (4.6 × 250 mm, Waters Instruments), at a mobile phase flow rate of 1 mL min^{-1} and using the same instrumentation as used above but with the wavelength set at 229 nm. The limit of detection was 0.25 μg mL^{-1}, and the linear peak area−concentration curve over the range 1−250 μg mL^{-1} had a correlation coefficient of 0.9997.

Biological Evaluation. *Intravenous Central Nervous System Delivery of Propofol.* Male 6-week-old MF1 mice were injected intravenously via the tail vein with various propofol formulations, and both the time to loss of righting reflex and the sleep time were recorded. The loss of righting reflex was confirmed in animals immediately after dosing by an animal failing to right itself when placed on its back, and animals which failed to sleep were recorded as having a sleep time of 0 min.

Topical Ocular Administration of Prednisolone. Male New Zealand White rabbits (n = 4, Harlan, U.K.) were dosed with prednisolone formulations (35 μL) into the lower cul de sac of each eye using an air displacement pipet. At 1, 2, and 4 h after dosing, animals were killed and the aqueous humor was sampled with a syringe. The vitreous humor was then collected, and all biological samples were immediately frozen

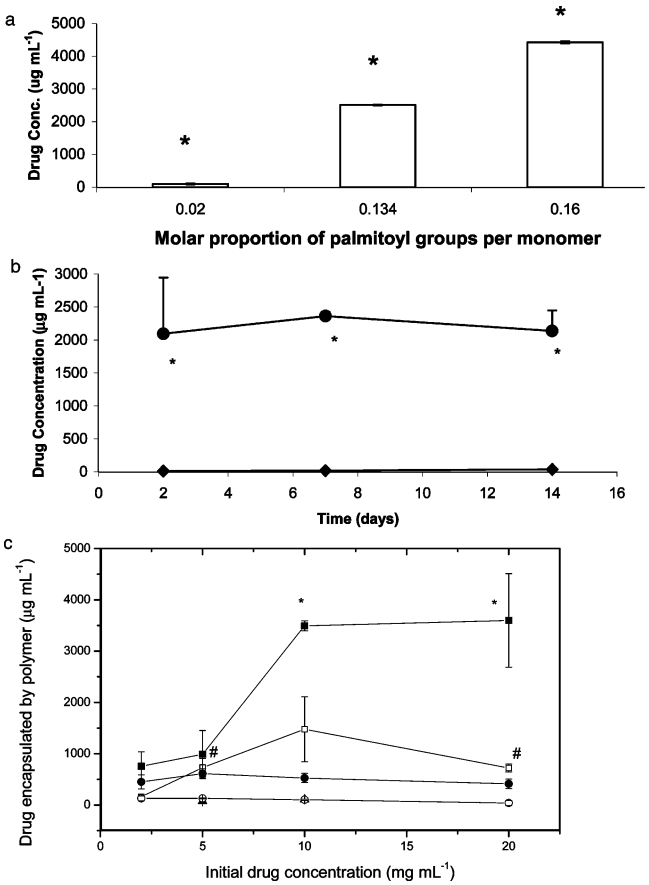

Figure 3. (a) Effect of palmitoylation levels on propofol encapsulation (mean ± sd): 0.02 molar proportion of palmitoyl groups = polymer C4; 0.134 molar proportion of palmitoyl groups = polymer C1; 0.16 molar proportion of palmitoyl groups = polymer C2; initial drug concentration = 10 mg mL^{-1}; initial polymer concentration = 5 mg mL^{-1}; asterisk = statistically significant difference ($p < 0.05$, $n = 4$); data represent mean ± sd. (b) Effect of palmitoylation on the encapsulation of propofol (mean ± sd): initial polymer concentration = 5 mg mL^{-1}; initial drug concentration = 10 mg mL^{-1}; ● = C1 + propofol; ◆ = C4 + propofol. For HI, approximate HLB, and cmc values (where available), see Table 1. An asterisk = statistically significantly different ($p < 0.05$). A 1 mol amount of C1 encapsulates 48 mol of propofol. Samples were stored at room temperature. (c) Effect of polymer molecular weight on drug encapsulation. Drug concentration was measured by HPLC after filtration (0.45 μm): ■ = C1 (5 mg mL^{-1}); □ = C1 (2.5 mg mL^{-1}); ● = D1 (5 mg mL^{-1}); ○ = D1 (2.5 mg mL^{-1}); △ = propofol in water; asterisk = statistically significant difference between polymers at a concentration of 5 mg mL^{-1}; △ = statistically significant difference between polymers at a concentration of 2.5 mg mL^{-1} ($p < 0.05$).

in liquid nitrogen. Samples of aqueous humor were thawed and analyzed by diluting 50 μL of aqueous humor with 150 μL of mobile phase containing the internal standard. These diluted samples were analyzed by HPLC as described above. Samples of vitreous humor (0.5 mL) were also thawed and extracted with ethyl acetate[35] prior to analysis.

Statistics. Statistical analysis was performed using the Students' *t*-test; significant differences were indicated by a *p* value of less than 0.05.

Results and Discussion

Synthesis of Carbohydrate Amphiphiles. Glycol chitosan (GC) samples of three molecular weights (Table 1), obtained by acid degradation, were used to prepare the amphiphilic polymers. Syntheses of quaternary ammonium palmitoyl glycol chitosan (GCPQ) samples (Figure 1) were confirmed by ^{1}H NMR[24] (0.90 ppm = CH_3 palmitoyl, 1.25 ppm = CH_2 palmitoyl, 1.60 ppm = CH_2 palmitoyl β to carbonyl, 22.5 ppm = CH_2 palmitoyl α to carbonyl, 3.02 ppm = CH_3 monomethyl and dimethyl amino, 3.12 ppm CH *C2* unsubstituted glycol chitosan, 3.35 ppm = CH_3 trimethylamino, 3.5−5.5 ppm = CH glycol chitosan). A total of 14 different amphiphiles were prepared with various levels of palmitoylation and quaternization (Table 1). Coarse control on palmitoylation levels was achieved by controlling the feed ratio of palmitic acid *N*-hydroxysuccinimide (PNS), while methyl quaternary ammonium levels largely remained similar so long as gravimetric methyl iodide/GC levels remained at 14.14 or below.

Self-Assembly. Polymer aggregation was probed with methyl orange[26,33] (Figure 2a), and the more hydrophobic polymers (HI = 1−2, HLB = 17−18) produced more stable aggregates, as evidenced by their low cmc's [<0.2 g L^{-1} (<10 μM), Figure 2a, Table 1]. The more hydrophobic polymers also produced more apolar hydrophobic cores as evidenced by the extent of the post micellization methyl orange hypsochromic shift (λ_{max} < 430 nm, Table 1). Polymer aggregates produced largely isotropic liquids at the concentrations studied (≤10 mg mL^{-1}). Aggregates in these isotropic liquids were 100−300 nm in diameter (Table 1), a size inconsistent with the unimolecular aggregation proposed by some authors.[36] Also both freeze fracture and negative stained transmission electron microscopy revealed a cluster of smaller 10−30 nm aggregates hierarchically organized into larger aggregates (Figure 2b,c), structures consistent with the model proposed in Figure 2d. This clustering arrangement is an unusual aggregate for amphiphilic polymers. Block copolymer micelles, for example, are conventional single micelle entities with a diameter of 12−36 nm,[14,15] and micelles prepared from cholesteryl pullulans are also believed to exist as single micelles of 25 nm in diameter.[16]

The molar cmc's of the current polymers when compared to cmc values recorded for other amphiphiles with even lower HLBs reveal that the current aggregates are more stable than other amphiphilic aggregates (Tables 1 and 2). The cmc's of the current polymers differ by 1−3 orders of magnitude from those recorded for the Pluronic block copolymer F127 (HLB = 14, cmc = 550 μM [6]) and polysorbate 20 (HLB = 16.7, cmc = 53 μM [4]). This more favorable aggregation phenomenon is consistent with the model proposed in Figure 2d as the ability of the polymer to form multiple inter- and intra-polymer hydrophobic and hydrogen bond associations would contribute to the entropy gain associated with the aggregation event in addition to the loss of water structure accompanying the micellization event. Additionally, an increase in molecular weight favors aggregation (Figure 2a), once again an observation consistent with the hypothesis that multiple inter- and intramolecular contacts stabilize the micelle clusters.

Drug Loading. The formation of more apolar domains favors hydrophobic drug encapsulation, and thus, the more hydrophobic polymers encapsulate greater amounts of drug (Figure 3a,b). Encapsulation levels are high: 5 mg mL^{-1} C2 (Table 1) encapsulates 4.43 ± 0.12 mg mL^{-1} propofol. The micellar clusters transformed to homogenously cloudy nanoparticle formulations on incorporation of drugs with a high log *P* such as propofol. Propofol resulted in the production of dense and larger particles from the micellar clusters which appeared as dense 50−200 nm particles on electron micrographs (Figure 4c). Prednisolone when added to polymer A7 (Table 1), however, resulted in isotropic (prednisolone concentration <0.5 mg mL^{-1}) or opalescent liquids (prednisolone concentration

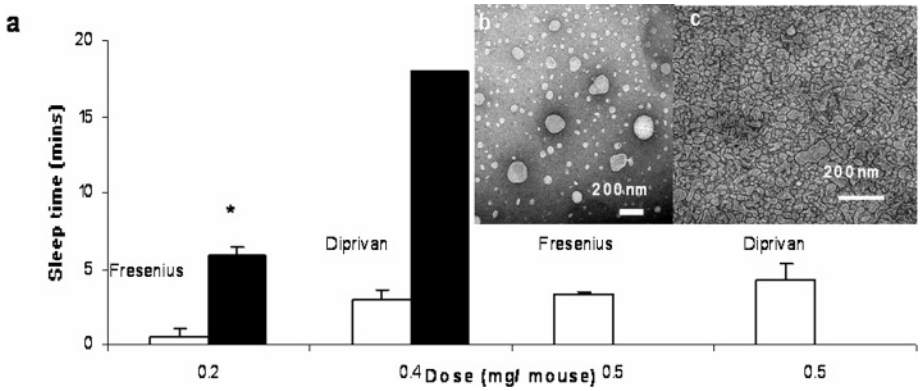

Figure 4. (a) Pharmacodynamic activity (sleep time, mean ± sd, $n \geq 4$) of propofol formulations after tail vein dosing to male MF1 mice. Mice were dosed as described: (i) 0.2 mg animals dosed with 0.2 mg of propofol in a 100 μL volume administered as either propofol emulsion (10 mg mL^{-1}, Fresenius, Germany) diluted to 2 mg mL^{-1} with phosphate-buffered saline (PBS, pH = 7.4) or a filtered GCPQ formulation (C1, 5 mg mL^{-1}, and propofol, 1.9 mg mL^{-1}, in PBS; pH = 7.4); (ii) 0.4 mg of animals dosed with 0.4 mg of propofol in a 100 μL volume administered as either Diprivan diluted in glycerol (0.24 M TEM of formulation shown in Figure 4b) to a concentration of 4 mg mL^{-1} or a filtered GCPQ formulation of propofol (C3, 5 mg mL^{-1}, propofol, 4.2 mg mL^{-1}, and lecithin, 2 mg mL^{-1}, in glycerol, 0.24 M, $n = 2$; TEM of formulation shown in Figure 4c); (iii) 0.5 mg of animals dosed with 0.5 mg of propofol administered in a 50 μL volume as either Diprivan (10 mg mL^{-1}) or propofol emulsion (Fresenius, 10 mg mL^{-1}). A loss of righting reflex time was only observed in animals receiving a low dose of the commercial emulsion formulations (0.37 ± 0.19 min in the 0.2 Fresenius animals). No sleep times were recorded in animals receiving the polymer alone. Asterisk = statistically significantly different ($p < 0.05$).

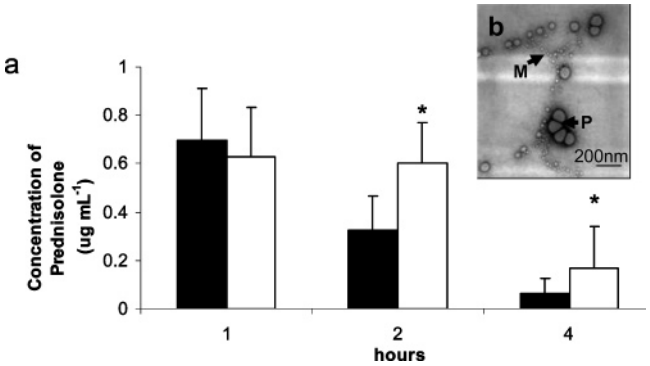

Figure 5. (a) Prednisolone concentrations (mean ± sd, $n = 4$) in the aqueous humor of rabbits dosed with either Prednisolone Forte (white bar, prednisolone acetate suspension, 10 mg mL^{-1}, 35 μL, Allergan, Irvine, CA) or a GCPQ formulation of prednisolone (black bar; A7, 1 mg mL^{-1}, 0.01 M $NaHCO_3$, and prednisolone, 1 mg mL^{-1}, 35 μL). Asterisk = statistically significant difference ($p < 0.05$, $n = 4$). (b) Negative stained transmission electron micrograph of prednisolone formulation; P = drug swollen particles, M = micellar clusters.

≤1.0 mg mL^{-1}) with particle sizes of 10−100 nm—a mixture of drug swollen particles and micellar clusters (inset Figure 5b).

The transformation of these carbohydrate amphiphile micellar clusters to dense nanoparticles on drug incorporation is thus illustrated with both C2 and A7 (Table 1). These exist as micellar clusters up to a concentration of at least 10 mg mL^{-1} (the highest concentration studied). C2 at a concentration of 5 mg mL^{-1} transforms into larger nonclustered dense particles (50−200 nm) in the presence of propofol (4.43 mg mL^{-1}) while A7 at a concentration of 1 mg mL^{-1} transforms to a mixture of micellar clusters and dense larger particles in the presence of prednisolone (1 mg mL^{-1}).

We have found that an increase in poly(ethylenimine) amphiphile aggregation number is seen in the presence of the hydrophobic molecule cholesterol,[26] and it is likely that the presence of a more hydrophobic drug shifts polymer aggregation from a micellar cluster to a more dense nanoparticle. Propofol levels in the carbohydrate formulations are stable for at least 14 days (Figure 3b). Table 3 shows that if ionization of the amine groups is suppressed by dialyzing the polymer against alkaline media, propofol encapsulation levels also increase. Removing the work associated with overcoming electrostatic repulsions, which dominate the early phase of the aggregation step, thus increases drug encapsulation levels.

The increase in drug encapsulation with increase in polymer hydrophobicity has been observed with block copolymers.[17,37] However, the formation of nanoparticles from micelle forming block copolymers or other amphiphiles in the presence of hydrophobic drugs has, to our knowledge, not been reported and hence is a novel feature of the current amphiphiles. For example propofol and F127 (1.78 mg mL^{-1} propofol and 40 mg mL^{-1} F127) form micelles that are 20−40 nm in diameter.[17]

In addition to polymer HLB/HI (Table 1, Figure 2a), polymer molecular weight also impacts on micelle stability. An increase in molecular weight increases micelle stability (Figure 2a). This can be seen by comparing polymers with the same HLB but differing molecular weight: polymers D1 and A2. This improvement in stability is reflected in the influence of molecular weight on drug encapsulation (Figure 3c). The drug/polymer molar ratio increases 10-fold with a 2.5-fold increase in molecular weight (Table 2). This observation is once again in agreement with the model proposed in Figure 2d, as multiple hydrophobic inter- and intramolecular contacts are only possible with a lengthy polymer chain.

These carbohydrate drug nanoparticles offer a key advantage over the block copolymers in that molar drug encapsulation levels are at least 1 order of magnitude higher with the current systems (Table 2 and Figure 3). We propose that these higher drug encapsulation levels are due to the nature of the aggregate: namely, the formation of a micellar cluster in excess of 100 nm in size as opposed to single micelles.

It is important to consider not only the efficiency of the amphiphile in incorporating hydrophobic materials into aqueous media but also the maximum level of drug incorporated into aqueous media—a clinically relevant parameter. The latter is also high compared to the block copolymer systems (Table 2). The exceptional drug loading achieved with these carbohydrate amphiphiles approaches 45% w/w, higher than that achieved with other polymeric particles loaded with hydrophobic drugs.[23,38,39] These particles are stabilized by the amphiphiles located on the surface of the particle which lower the interfacial energy associated with the particle.

Table 3. Effect of Polymer Surface Charge on Propofol Encapsulation

disperse phase	drug concn (mg mL^{-1}) encapsulated in C1 (5 mg mL^{-1}) dialyzed against sodium chloride solution (0.1 M) and water with init drug concn = 10 mg mL^{-1}, mean ±sd (n = 4)	drug concn encapsulated in C1 (5 mg mL^{-1}) dialyzed against alkaline sodium chloride solution (sodium chloride = 0.1 M, sodium bicarbonate = 0.01 M) with init drug concn = 10 mg mL^{-1}, mean ±sd (n = 4)
	1.52 ± 0.47	3.45 ± 0.02[a]
phosphate-buffered saline (pH = 7.4)	1.32 ± 0.07	2.16 ± 0.04[a]
glucose (5% w/v)	0.35 ± 0.05	1.75 ± 0.04[a]

[a] Statistically significant difference between alkaline and neutral dispersions ($p < 0.05$).

Previous studies on hydrophobised carbohydrates have focused on their viscosity enhancing properties,[40−42] their ability to form gels[24,43] and aqueous insoluble aggregates.[16,25,27,44−47] With respect to water-soluble carbohydrate amphiphile aggregates,[24,25,36] characterization of their ultrastructure and/ or bioavailability enhancing effects have not been reported. Here we show that the aggregation behavior involves a hierarchical organization of micelles into self-repellent colloidal clusters for the first time with direct micrograph evidence supported by dynamic light scattering evidence.

Bioavailability Enhancement with Carbohydrate Drug Carriers. Figures 4 and 5 present data on the transport of drugs across biological barriers with these new carbohydrate particles. Drug bioavailability is enhanced quite significantly using these carbohydrate formulations. Two model drugs were chosen: the ocular antiinflammatory drug prednisolone and the intravenous anaesthetic propofol. On topical application to the eye, aqueous humor levels with 0.035 mg of prednisolone formulated with the carbohydrate amphiphiles are statistically indistinguishable at early time points from drug levels obtained using 0.35 mg of prednisolone in Prednisolone Forte. Dilution of Prednisolone Forte was not carried out so as not to destabilize the formulation. No drug was detected with any of the prednisolone formulations in the vitreous humor. These carbohydrate nanoparticles facilitate drug absorption across the cornea to the aqueous humor but fail to deliver drug to the back of the eye. However this is unsurprising in view of the topical mode of delivery and characteristics of the drug.[48]

The sleep times obtained with the carbohydrate propofol formulations are up to 10 times those obtained when using either the commercial Fresenius or Diprivan formulations. A loss of righting reflex time could not be recorded with the GCPQ formulations as animals were asleep by the end of the injection administration period (see legend of Figure 4); evidence that delivery of the centrally acting drug across the blood brain barrier is rapid and efficient. To compare the formulations, the amount of propofol giving rise to each minute of sleep time were compared: values were 0.426 and 0.032 mg min^{-1} with 0.2 mg of propofol/mouse (0.1 mL of dose volume) of the Fresenius and C1 formulations, respectively, 0.134 and 0.023 mg min^{-1} with 0.4 mg of propofol/mouse of the Diprivan and C3 formulations, respectively (0.1 mL of dose volume), and 152 and 111 mg min^{-1} with 0.5 mg of propofol/mouse with the undiluted (10 mg mL^{-1}) Fresenius and Diprivan formulations, respectively (0.05 mL of dose volume). While this strategy may offer anaesthetic induction benefits to propofol as rapid induction is desirable,[49] principally these experiments demonstrate that this technology may prove beneficial for the CNS (central nervous system) delivery of behavior modification therapies or therapies to treat specific brain diseases.

From the current study, the mechanism by which these carbohydrate amphiphiles improve drug delivery to the CNS or indeed across the cornea is not fully understood; however, with respect to the CNS, some indicators may be found in an analysis of the physical properties of the formulations. The particle size and particle size distribution of the commercial propofol formulation, as exemplified with Diprivan (Figure 4b), is larger than that seen with the carbohydrate formulation (Figure 4c). The formulations shown in Figure 5b,c were filtered; however, unfiltered carbohydrate formulations show no bioavailability efficiency gains when compared to the commercial emulsion formulations (data not shown). Since filtration of polymer aggregates results in a decrease in particle size (Table 1), we hypothesise that the reduced particle size is responsible in part for the drug delivery activity of these carbohydrate nanoparticles.

Furthermore lipid free formulations of propofol have been reported to be accompanied by an increase in potency,[50] presumably due to a lack of a lipid reservoir in the blood which would favor partitioning into the brain. It is possible that the lack of a lipid reservoir in the blood with the carbohydrate formulations is also responsible for the increased potency of this formulation observed here.

In conclusion, carbohydrate amphiphiles have been synthesized and found to self-assemble into micellar clusters which provide an enhanced carrying capacity for hydrophobic drug molecules and facilitate the transport of drug molecules across biological barriers, thus enhancing their bioavailability. The current technology offers a solution to pharmaceutical formulators of hydrophobic drugs and further testing is warranted.

Acknowledgment. This work was funded by grants from Scottish Enterprise Glasgow, The Engineering and Physical Sciences Research Council of the United Kingdom, and Allergan, Irvine, CA.

References and Notes

(1) Kilpatrick, P. *Nat. Drug Discovery* **2003**, *2*, 337.
(2) Wenlock, M. C.; Austin, R. P.; Barton, P.; Davis, A. M.; Leeson, P. D. *J. Med. Chem.* **2003**, *46*, 1250−1256.
(3) Rowe, R. C.; Sheskey, P. J.; Weller, P. J. *Handbook of Pharmaceutical Excipients*; Pharmaceutical Press: London, 2003.
(4) Florence, A. T.; Attwood, D. *Physicochemical Principles of Pharmacy*; Macmillan Press: Basingstoke, U.K., 1998.
(5) Cheng, H. Y.; Holl, W. W. *J. Pharm. Sci.* **1990**, *79*, 907−912.
(6) Alexandridis, P.; Holzwarth, J. F.; Hatton, T. A. *Macromolecules* **1994**, *27*, 2414−2425.
(7) Nam, Y. S.; Kang, H. S.; Park, J. Y.; Park, T. G.; Han, S. H.; Chang, I. S. *Biomaterials* **2003**, *24*, 2053−2059.
(8) Krishna, A. K.; Flanagan, D. R. *J. Pharm. Sci.* **1989**, *78*, 574−576.
(9) Strickley, R. G. *Pharm. Res.* **2004**, *21*, 201−230.
(10) Trapani, G.; Lopedota, A.; Franco, M.; Latrofa, A.; Liso, G. *Int. J. Pharm.* **1996**, *139*, 215−218.
(11) Arnanson, T.; Elworthy, P. H. *J. Pharm. Pharmacol.* **1980**, *32*, 381−385.
(12) Ong, J. T. H.; Manoukian, E. *Pharm. Res.* **1988**, *5*, 704−708.
(13) Shuai, X.; Ai, H.; Nasongkla, N.; Kim, S.; Gao, J. *J. Controlled Release* **2004**, *98*, 415−426.
(14) Kabanov, A. V.; Batrakova, E. V.; Meliknubarov, N. S.; Fedoseev, N. A.; Dorodnich, T. Y.; Alakhov, V. Y.; Chekhonin, V. P.; Nazarova, I. R.; Kabanov, V. A. *J. Controlled Release* **1992**, *22*, 141−158.
(15) Yu, B. G.; Okano, T.; Kataoka, K.; Kwon, G. *J. Controlled Release* **1998**, *53*, 131−6.
(16) Akiyoshi, K.; Deguchi, S.; Moriguchi, N.; Yamaguchi, S.; Sunamoto, J. *Macromolecules* **1993**, *26*, 3062−3068.
(17) Dwyer, C.; Viebke, C.; Meadows, J. *Colloids Surf., A* **2005**, *254*, 23−30.

(18) Kwon, G. S.; Kataoka, K. *Adv. Drug Delivery Rev.* **1995**, *16*, 295−309.
(19) Allen, C.; Maysinger, D.; Eisenberg, A. *Colloids Surf., B* **1999**, *16*, 3−27.
(20) Jones, M. C.; Leroux, J. C. *Eur. J. Pharm. Biopharm.* **1999**, *48*, 101−111.
(21) Torchilin, V. P. *J. Controlled Release* **2001**, *73*, 137−172.
(22) Savic, R.; Luo, L.; Eisenberg, A.; Maysinger, D. *Science* **2003**, *300*, 615−618.
(23) Francis, M. F.; Lavoie, L.; Winnik, F. M.; Leroux, J. C. *Eur. J. Pharm. Biopharm.* **2003**, *56*, 337−346.
(24) Uchegbu, I. F.; Sadiq, L.; Arastoo, M.; Gray, A. I.; Wang, W.; Waigh, R. D.; Schätzlein, A. G. *Int. J. Pharm.* **2001**, *224*, 185−199.
(25) Miwa, A.; Ishibe, A.; Nakano, M.; Yamahira, T.; Itai, S.; Jinno, S.; Kawahara, H. *Pharm. Res.* **1998**, *15*, 1844−1850.
(26) Wang, W.; Qu, X.; Gray, A. I.; Tetley, L.; Uchegbu, I. F. *Macromolecules* **2004**, *37*, 9114−9122.
(27) Wang, W.; McConaghy, A. M.; Tetley, L.; Uchegbu, I. F. *Langmuir* **2001**, *17*, 631−636.
(28) Discher, D. E.; Eisenberg, A. *Science* **2002**, *297*, 967−973.
(29) Wang, W.; Tetley, L.; Uchegbu, I. F. *Langmuir* **2000**, *16*, 7859−7866.
(30) Gref, R.; Minamitake, Y.; Peracchia, M. T.; Trubetskoy, V. S.; Torchilin, V. P.; Langer, R. *Science* **1994**, *263*, 1600−1603.
(31) Furusaki, E.; Ueon, Y.; Sakairi, N.; Nishi, N.; Tokura, S. *Carbohydr. Polym.* **1996**, *29*, 29−34.
(32) Griffin, W. C. *J. Soc. Cosmet. Chem.* **1949**, *1*, 311
(33) Wang, G. J.; Engberts, J. *J. Org. Chem.* **1994**, *59*, 4076−4081.
(34) Kan, P. L.; Papahadjopoulos-Sternberg, B.; Wong, D.; Waigh, R. D.; Watson, D. G.; Gray, A. I.; McCarthy, D.; McAllister, M.; Schatzlein, A. G.; Uchegbu, J. F. *J. Phys. Chem. B* **2004**, *108*, 8129−8135.
(35) Rocci, M. L.; Jusko, W. J. *J. Chromatogr.* **1981**, *224*, 221−227.
(36) Yoshioka, H.; Nonaka, K.; Fukuda, K.; Kazama, S. *Biosci. Biotechnol. Biochem.* **1995**, *59*, 1901−1904.
(37) Rekatas, C. J.; Mai, S.-M.; Crothers, M.; Quinn, M.; Collett, J. H.; Attwood, D.; Heatley, F.; Martini, L.; Booth, C. *Phys. Chem. Chem. Phys.* **2001**, *3*, 4769−4773.
(38) Kim, S. Y.; Lee, M. Y. *Biomaterials* **2001**, *22*, 1697−1704.
(39) Francis, M. F.; Piredda, M.; Winnik, F. M. *J. Controlled Release* **2003**, *93*, 59−68.
(40) Landoll, L. M. *J. Polym. Sci., Polym. Chem. Ed.* **1982**, *20*, 443−455.
(41) Kjoniksen, A. L.; Nystrom, B.; Iversen, C.; Nakken, T.; Palmgren, O.; Tande, T. *Langmuir* **1997**, *13*, 4948−4952.
(42) Philppova, O. E.; Volkov, E. V.; Sitnikova, N. L.; Khokhlov, A. R.; Desbrieres, J.; Rinaudo, M. *Biomacromolecules* **2001**, *2*, 483−490.
(43) Noble, L.; Gray, A. I.; Sadiq, L.; Uchegbu, I. F. *Int. J. Pharm.* **1999**, *192*, 173−182.
(44) Wakita, M.; Hashimoto, M. *Kobun. Ronbun.* **1995**, *52*, 589−593.
(45) Uchegbu, I. F.; Schatzlein, A. G.; Tetley, L.; Gray, A. I.; Sludden, J.; Siddique, S.; Mosha, E. *J. Pharm. Pharmacol.* **1998**, *50*, 453−8.
(46) Lee, K. Y.; Jo, W. H.; Kwon, I. C.; Kim, Y. H.; Jeong, S. Y. *Langmuir* **1998**, *14*, 2329−2332.
(47) Kwon, S.; Park, J. H.; Chung, H.; Kwon, I. C.; Jeong, S. Y.; Kim, I. S. *Langmuir* **2003**, *19*, 10188−10193.
(48) Hughes, P. M.; Olejnik, O.; Chang-Lin, J. E.; Wilson, C. G. *Adv. Drug Delivery Rev.* **2005**, *57*, 2010−2032.
(49) Langley, M. S.; Heel, R. C. *Drugs* **1988**, *35*, 334−372.
(50) Dutta, S.; Ebling, W. F. *J. Pharm. Pharmacol.* **1998**, *50*, 37−42.

BM0604000